

waterloopkundig laboratorium  
delft hydraulics laboratory

an artificial ceiling for free surface flow  
reproduction in scale modelling of local scour

P.A. Kolkman

publication no. 283

November 1982

BIBLIOTHEEK  
Dienst Weg- en Waterbouwkunde  
Van der Burghweg  
Postbus 5044, 2600 GA Delft  
Tel. 015 - 699111

---

an artificial ceiling for free surface flow  
reproduction in scale modelling of local scour

P.A. Kolkman

presented at the International Conference on the  
Hydraulic Modelling of Civil Engineering Structures,  
Coventry, England, September 22/24, 1982

---

publication no. 283

November 1982

**BIBLIOTHEEK**  
Dienst Weg- en Waterbouwkunde  
Van der Burghweg  
Postbus 5044, 2600 GA Delft  
Tel. 015 - 699111

**27 MEI 1993**



# Hydraulic Modelling of Civil Engineering Structures

Coventry, England: September 22-24, 1982

## AN ARTIFICIAL CEILING FOR FREE SURFACE FLOW REPRODUCTION IN SCALE MODELLING OF LOCAL SCOUR

P. A. Kolkman

Delft Hydraulics Laboratory, The Netherlands  
(Senior Research Officer, Delft University of Technology)

### Summary

When hydraulic model research is done for scour behind structures a conflict can occur between the demands of Froude similarity and the minimum water velocity which is needed in the model to study erosion.

This problem could be solved by covering the free water surface with a ceiling which follows the water surface at Froude similitude conditions. When the water velocity is increased (Froude number exaggeration) the flow pattern will remain conform to the Froude similitude condition.

This paper describes two-dimensional erosion experiments, in which the sediment is reproduced by polystyrene grains, at conditions where the Froude number exaggeration in the normal condition results in a change of flow pattern and erosion characteristics. The tests with a ceiling indeed tend to confirm the principles of this device. The following investigated parameters are discussed: velocity distribution (average and r.m.s. value), two parameters related to time scaling, the initial slope and the location of the deepest point of the scour hole.

Held at the University of Warwick, Coventry

Organised and sponsored by  
BHRA Fluid Engineering, Cranfield, Bedford MK43 0AJ, England

© BHRA Fluid Engineering 1982

NOMENCLATURE

|                  |   |              |
|------------------|---|--------------|
| $d$              | = grain diameter of soil or rip-rap                     | m or mm      |
| $h_o$            | = waterdepth at the end of the downstream protection    | m            |
| $h_m$            | = maximum depth of scour hole                           | m            |
| $t$              | = time  | hrs          |
| $u$              | = watervelocity at the end of the downstream protection | $m\ s^{-1}$  |
| $\bar{u}$        | = depth averaged value of $u$                           | $m\ s^{-1}$  |
| $\bar{u}_{cr}$   | = value of $\bar{u}$ where movement of grains start     | $m\ s^{-1}$  |
| $x$              | = location of deepest point of scour hole               | m            |
| $z$              | = height above the bed protection                       | m            |
| $T_l$            | = time needed to reach a $h_m$ value equal to $h_o$     | hrs          |
| $\alpha$         | = dimensionless coefficient                             |              |
| $\beta$          | = upstream slope angle of scour hole                    |              |
| $\gamma$         | = dimensionless coefficient                             |              |
| $\Delta$         | = $(\rho_s - \rho_w)/\rho_w$                            |              |
| $\rho_s$         | = density of soil grains                                | $kg\ m^{-3}$ |
| $\rho_w$         | = density of water                                      | $kg\ m^{-3}$ |
| $\sigma$         | = turbulence intensity (root mean square value)         | $m\ s^{-1}$  |
| $\bar{\sigma}$   | = depth averaged value of $\sigma$                      | $m\ s^{-1}$  |
| $\xi_{\Delta h}$ | = head loss coefficient                                 |              |

## 1. INTRODUCTION

When a prototype condition of fine loose material has to be investigated for scour problems in a scale model, at the Delft Hydraulics Laboratory polystyrene grains are applied. These are easily transported by the flow and move, due to the low density, easily in suspension. For flow conditions with Froude-numbers much smaller than unity (a nearly horizontal water surface) a great number of systematic scale tests with varied properties of the erodable material have resulted in the establishment of empiric relations for the development of scour holes. Some parameters which are still dependent of the geometry of the construction and the length and roughness of the bottom protection can, for a certain construction, be investigated in a special purpose scale model with erodable bed. These parameters concern the time scaling and the shape (especially the upstream slope) of the scour hole. The downstream slope is not reproduced adequately. Recently tests were performed in prototype conditions which largely confirmed these relations, with the exception of the upstream slope which in the long term became steeper. This investigation has been published by de Graauw and Pilarczyk (Ref. 1).

For the application of these relations in scale model research one can apply the velocity scale arbitrarily under conditions where the velocity is greater than  $\bar{u}_{crit}$ , and the water-level also in the model is nearly horizontal (low Froude-number in the model).

Remark:  $\bar{u}$  is introduced as a depth averaged velocity.

The velocity in the model is so chosen that within a reasonable amount of time (for instance 1 to 4 hours) a scour hole develops with a depth equal to the initial water depth. This means that in general the velocity exceeds the one conform to the Froude scaling. In this paper an investigation is presented where the following idea is checked. Suppose there is a condition where the velocity exaggeration compared to the Froude scaling results in an undulated and non-horizontal water-level and hence in a unacceptable flow pattern. If the "correct" water-level was fixed by means of an artificial ceiling, it should be possible to exceed the Froude similitude velocity without changing the flow pattern, and are the scouring relations now maintained?

This investigation can then result in greater freedom in the velocities applied in a model and also of the choice of bed materials more difficult to erode. Moreover it gives the possibility to do a more systematic scour research in a closed tunnel circuit also for higher Froude-number conditions of free surface flow.

## 2. THE PARAMETERS WHICH ARE INVESTIGATED

Preliminary to the erosion test the velocity and turbulence distribution over the depth, especially at the end of a bottom protection were studied for a two-dimensional free surface condition. This was done at low velocity - say Froude-scaled - conditions and with an exaggerated velocity where the flow pattern was modified. This was then repeated but with the application of a ceiling. The final tests were then performed with erodable material to establish the scouring relations (shape of scour hole and depth-time relationship).

The shape of the scour hole, as far as this is relevant for the stability of the structure, can be described by the upstream slope ( $\cotg \beta$ ) and by the location of the deepest point ( $x/h_{max}$ ). It appears that, apart from the initial scouring, both values do not vary much during the scouring process when only one geometry is considered at a low Froude number condition.

The rate of scouring is related to the time  $T_1$  (in hrs) needed to reach a depth of one time the initial water depth, see Ref. 3.

$$T_1 = 250 \Delta^{1.7} h_o^2 / (\alpha \bar{u} - \bar{u}_{cr})^{4.3} \quad (1)$$

$\alpha$  is only dependent of the configuration of the structure and the length and roughness of the bottom protection.  $h_o$  and  $\bar{u}$  are both defined at the end of the bottom protection.  $\Delta = (\rho_s - \rho_w) / \rho_w$  in which  $\rho_s$  = density of the sediment grains. The rate of scouring at a different time  $t$  is determined by the relation



$$\frac{h_{\max}}{h_0} = \left( \frac{t}{T_1} \right)^\gamma \quad (2)$$

It appears, see Ref. 3, that at a two-dimensional condition  $\gamma = 0.38$ , nearly independent of the structures geometry. For a three-dimensional condition  $\gamma$  has to be determined in a scale model.

Remark:

The factor 250 in (1) was recently modified into 330 after a re-examination available tests, but in this paper still 250 is applied.

In this investigation all parameters are studied which are dependent of geometry and length and roughness of the bottom protection. Included is the rate of turbulence  $\sigma$ , which was related to the depth averaged velocity  $\bar{u}$ .

The investigated parameters were:

- $u/\bar{u}$  at the end of the protection
- $\sigma/\bar{u}$  at the end of the protection
- $\bar{\sigma}/\bar{u}$  at the end of the protection
- $\cotg \beta$
- $x/h_m$
- $\alpha$

### 3. THE TESTED GEOMETRIES

The investigated two-dimensional geometry was originally related to a caisson-type barrage with a grid gate, see Ref. 2. This gate was placed symmetrically on the caisson which was stabilized at both sides with a rock-fill embankment.

This resulted in a test condition with a low rectangular caisson, 0.2 m high and 1 m wide in the flow direction. The two rock fill side slopes were 1:5 with a bottom protection at both sides of 3.5 m length. For the two latter test series the bottom protection was shortened to 2 m to obtain more pronounced differences for conditions without and with a ceiling.

For the used schematization see further Fig. 1.

In a second configuration a rib of 0.08 m high was taken which in fact is a short crested weir. This rib was also placed symmetrically on the caisson.

The rock-fill slopes and the bottom protection consisted of broken stones,  $d_{50} = 15$  mm.

### 4. TEST INSTALLATION, SOIL AND EQUIPMENT

The investigation took place in a 0.8 m wide flume, 22 m in length and 1.2 m deep. The erodible bed material consisted of polystyrene with a uniform grain size of 2.6 mm and a density of 1035 kg/m<sup>3</sup>, so  $\Delta = 0.035$ .

By placing the upstream bottom protection at the upstream flume end, it was possible to provide a polystyrene layer of 0.6 m thickness and 6 m length. At the downstream end of this layer a weak slope was applied ending on the bottom of the flume. At the flume end a polystyrene filter was placed to prevent recirculation of the grains; only clear-water erosion was tested.

To measure the velocity and turbulence, use was made of the DHL Current-Flow Meter equipment. The propellor, with a diameter of 15 mm, was equipped with a bi-directional electrode detection,  $u_{\min} = 0.025$  m/s. A Saycor correlator and probability analyser was used for the  $\sigma$  determination. The head difference over the construction and the water-level surface curve was measured by point gauges.

The scour hole profiles were measured with the DHL Profile-Indicator (called Provo), type MK V which, by means of a servo system, keeps a constant distance from the bottom (principle based on change of conductivity due to bottom influence): sensitivity to bed level changes greater than the used grain diameter. By applying an X-Y steered carriage a number of cross-sections could be determined in a short time.

Remark:

From other investigations it was known that in a wider flume a pure two-dimensional

scour hole is never obtained. This is due to spiral currents induced at the upstream end of the scour hole. The width-averaged scour hole profile is however comparable with results of flumes with a smaller width.

## 5. RESULTS OF THE PRELIMINARY INVESTIGATION

Preliminary to the erosion tests the interesting range of Froude numbers was established in a smaller flume (with a fixed bottom) and the first experience of the influence of a ceiling on the flow pattern was obtained.

To start with, the rib configuration was investigated. This was simpler than the grid because the ceiling remains free from the rib and its position could easily be changed. It appeared that a practical range of velocities at the end of the bottom protection was 0.18 m/s to 0.4 m/s in combination with a water depth of 0.4 m. At 0.2 m/s there is still subcritical flow. The water surface profile is indicated in Fig. 2. The flow pattern shows a bottom eddy above and past the downstream slope. At higher velocities a hydraulic jump tends to form (also Fig. 2) and the flow now remains attached to the slope. Also it appeared that the flow needs a greater length before the flow profile reaches its equilibrium shape related to the roughness of the bottom protection.

Then a ceiling was designed to fix the water surface profile to the  $\bar{u} = 0.2$  m/s condition (attention: the ceiling shapes of the preliminary investigation are not shown in the figures of this paper). The ceiling reached to 0.5 m downstream of the rib; at that distance for all free surface tests, the water-level reached about the level value further downstream. Upstream a short length of 0.1 m was applied. A short ceiling is supposed to have the advantage of low additional friction.

It appeared that with exaggerated velocities ( $\bar{u} > 0.2$  m/s) low pressures occur under the ceiling which result in air suction. So it can be concluded that the ceiling needs to be airtight, that air suction through vortices should be prevented and that a transparent ceiling is advisable to check the absence of air. Due to water-level fluctuations air was also entrapped from the downstream side.

For the final tests a longer upstream part of the ceiling was used to reduce the risk of air suction; also a larger radius of the roundings of the edges was then applied (Fig. 3, situation of series III).

The result of the ceiling was favourable in the sense that exaggerated values of the velocities did not result in a change of flow pattern. An extra head difference over the weir due to the ceiling was present but was judged to be acceptable.

A test series then followed with the grid. For the free surface profiles see again Fig. 2. At the lower velocities (again  $\bar{u} = 0.2$  m/s at the end of the protection) the water-level difference over the grid appeared as a steep jump. This only influenced the velocity profile locally. The redistribution of the velocities over the flume depth took place gradually and this resulted in a downward velocity component over a long distance. Again a hydraulic jump occurred at higher velocities, and downstream of it the discharge was more or less evenly distributed over the depth. But again it took a longer distance before the equilibrium velocity profile was reached. The application of a ceiling adapted to the  $\bar{u} = 0.2$  m/s condition resulted again in an independence of the flow pattern from the  $\bar{u}$  value. The other experiences with the ceiling were also the same as with the rib configuration. Only the  $\bar{u} = 0.2$  m/s condition with ceiling resulted in a too low velocity near the water surface, probably due to a friction effect. Related to this the bottom velocities were a little too high. Various tests were then performed with a varied height position of the ceiling to see how the bottom velocity was effected, but this risks disturbing the whole flow pattern too much. Some improvement was obtained by tilting the ceiling a little and keeping the level at the downstream end the same. When the upstream part is lifted somewhat the resulting converging flow has a smaller boundary layer effect near the ceiling. The risk is however that the boundary layer above the bottom protection is also affected.

The length of the ceiling at the downstream end was then enlarged from 0.5 to 1.25 m (up to the beginning of the rounding of the downstream edge). The velocity profile remained conform to the 0.2 m/s condition without ceiling, the total resistance over the construction again increased somewhat. At velocities strongly exceeding the 0.2 m/s



value the head difference with ceiling is smaller than without due to the absence of a hydraulic jump. This elongated ceiling had a weak slope (1:8.2) just downstream of the grid instead of the jump of the water-level at the grid which occurred at the Froude similarity flow. This was also done to eliminate the local velocity reduction near the ceiling. The two effects, the elongation and the weak slope, were not tested separately. The air entrapment from downstream had disappeared. It was found for all ceiling tests that at a velocity exaggeration the level of the ceiling did not correspond anymore to the neighbouring free water surfaces (due to an increase of the water-level slope above the bed protection and an increased head difference over the ceiling). Careful design of the upstream and downstream ceiling end is necessary.

### Conclusions

It was concluded from the preliminary investigations that for the scouring tests a moderately elongated ceiling should be applied, constructed of perspex. The steep jump at the water-level difference over the grid should be applied at one variant and the weaker step at another (Fig. 3, ceiling of series I and II). For the tests with the grid the ceiling ends should consist of planes under a 45° slope. (At the upstream end of inlet structures this slope is in general experienced to be an optimum to prevent air suction). For the rib-configurations however it was decided to round only the ceiling edges (see also Fig. 3).

## 6. RESULTS OF THE SCOURING TESTS

The test programme consisted of three series:

- I The condition with the grid with the long bottom protection of 3.5 m, being the condition which most resembled the original grid gate investigation referred to in Par. 3. All tests were done without ceiling and with a ceiling based on the  $\bar{u} = 0.2$  m/s condition. The tests with ceiling were done with a nearly stepwise change in level to represent the level difference over the grid. The configuration and position of the ceiling is found in Fig. 3. The small dip in the downstream water-level at the  $\bar{u} = 0.2$  m/s condition was not reproduced.
- II The same grid as series I but with a shorter bottom protection (2 m). The ceiling had a weak slope to represent the water-level difference over the grid. Apart from minor details the ceiling was similar to the one of series I (Fig. 3).
- III The rib configuration was tested with a ceiling having quarter circular roundings at the upstream and downstream ends, ending in a vertical wall. The dip in the downstream water-level at the  $\bar{u} = 0.2$  m/s condition was fully reproduced in the ceiling shape. In this series the length of the bottom protection was again 2 m.

For all tests the downstream water depth was fixed on  $h_0 = 0.4$  m and the tests with a ceiling had a ceiling height at the same level. The reference velocity on which the ceiling shape was designed was  $\bar{u} = 0.2$  m/s.

Both  $h_0$  and  $\bar{u}$  were defined at the downstream end of the bottom protection.

The critical scouring velocity was determined;  $\bar{u}_{cr} = 0.09$  m/s. All investigated parameters are summarized in Par. 2.

Table I shows all data of the different test runs, and Table II summarizes the results concerning duration of scouring and shape of the scour hole. These quantities are established at the moment that the scour depth  $h_m$  equals the initial water depth  $h_0$ . The quantities are all width-averaged values.

Figure 5 shows all velocity ( $u$ ) and turbulence ( $\sigma$ ) profiles at the end of the bottom protection. The depth averaged value of  $\sigma/\bar{u}$ , being  $\bar{\sigma}/\bar{u}$  is given in Table II together with the head difference over the structure measured at the extremes of the upstream and downstream bottom protection. To check whether the ceiling tests result in a constant head loss coefficient, the coefficient  $\xi_{\Delta h}$  is also calculated

$$\xi_{\Delta h} = 2g\Delta h/\bar{u}^2 \quad (3)$$

The quantities of Table II, which are related to the scouring ( $\alpha$ ,  $\cotg \beta$  and  $x/h_{max}$ ),



and the  $\bar{\sigma}/\bar{u}$  value are plotted in Fig. 6. In each graph the reference level is plotted related to the  $\bar{u} = 0.2$  m/s condition without ceiling. This reference level is indicated by the index  $F_r$ , because the ceiling aims to fix the water-level and flow pattern of a Froude-scaled prototype condition.

The test results are summarized as follows:

- a. Concerning air suction: none of the ceilings gave suction problems.
- b. Concerning the velocity and turbulence profile at the end of the bottom protection (Fig. 5): the situation with ceiling gave a strongly reduced sensitivity for the applied  $\bar{u}$  value; the  $u$  and  $\sigma$  profile with ceiling correspond more or less to the reference condition. The influence of the steepness of the water-level jump at the grid gate was not measurable.
- c. The relative depth-averaged turbulence level ( $\bar{\sigma}/\bar{u}$ ) was quite improved by applying the ceiling (Fig. 6), although in the situation of series II somewhat less.
- d. Concerning the head difference over the structure (Table II): the results are scattered, but it is seen that the application of the ceiling results in an increase of head difference, particularly in the situation of series III. In these tests the velocity range was smaller than in the preliminary tests, and it was not found back that at higher velocities the application of a ceiling can reduce the head difference.
- e. The time  $T_1$  needed to reach a scour depth equal to  $h_0$ : the ceiling acts satisfactorily in keeping the  $\alpha$  value constant and equal to its reference level.
- f. The upstream slope of the scour hole: Fig. 6 shows that in general the ceiling works in the right sense but at the situation of series II the result is not completely satisfactory.
- g. The location of the deepest point of the scour hole: although the results remain somewhat scattered there is a clear functioning of the ceiling, the situation of series II but is less satisfying.

## 7. CONCLUSIONS

In general the effect of the ceiling satisfies the expectation that the flow pattern remains fixed so that the relations of Eq. (1 and 2), which apply to low Froude numbers, can be applied in models with an exaggerated velocity compared to the Froude similitude. The somewhat poorer results of situation 2 warrants the conclusion that the realistic step in the ceiling level to reproduce the water-level difference over the grid is certainly not worse than the weak slope transition. Concerning future research; it would be of interest to know whether the relations of Equations (1) and (2) are also applicable to high Froude number conditions, wherein however  $\alpha$ ,  $\cotg \beta$  and  $\gamma$  will become dependent on the Froude number. The results of this investigation open the possibility of performing more systematic erosion tests in a closed water tunnel. At higher velocities even bottom material with a prototype density can be applied.

### Acknowledgement:

I wish to express my gratitude to two persons; this research work was undertaken 5 years ago and since then the experimenters have left our Institute. They have therefore not been able to cooperate on this paper. I refer to H. Depeweg, at that time Project engineer in our branch and H. van Wieringen who used this investigation for his Master Thesis.

### REFERENCES

1. De Graauw, A.F.F. and Pilarczyk, K.: "Model-Prototype Conformity of Local Scour in Non-Cohesive Sediments beneath an Overflow Dam". Publication 242 of Delft Hydraulics Lab, also published in 19th IAHR Congress, N. Delhi Febr. 1981 paper Da 2.
2. De Jong, R.J.: "Excitation and Vibration of a Grid Gate" paper C8 in IAHR/IUTAM symposium (1979) on Practical Experiences with Flow-Induced Vibrations, Editor E. Naudascher, Springer Verlag.
3. Breusers, H.C.N. and Schukking, W.H.P.: "Systematisch onderzoek naar twee- en driedimensionale ontgraving" research report Delft Hydr. Lab. M648/863.

TABLE I : TEST PROGRAM

| test nr.          | configuration     | ceiling | length downstream bottom protection | average velocity $\bar{u}$ [m/s] |
|-------------------|-------------------|---------|-------------------------------------|----------------------------------|
| series I<br>T17   | grid 14/17        | without | 3,5 m                               | 0,23                             |
|                   | grid 14/17        | without | 3,5 m                               | 0,34                             |
| T19               | grid 14/17        | with    | 3,5 m                               | 0,22                             |
|                   | grid 14/17        | with    | 3,5 m                               | 0,35                             |
| series II<br>T21  | grid 14/17        | without | 2 m                                 | 0,23                             |
|                   | grid 14/17        | without | 2 m                                 | 0,35                             |
| T23               | grid 14/17        | with    | 2 m                                 | 0,22                             |
|                   | grid 14/17        | with    | 2 m                                 | 0,35                             |
| series III<br>T25 | rib configuration | without | 2 m                                 | 0,19                             |
|                   | rib configuration | without | 2 m                                 | 0,22                             |
|                   | rib configuration | without | 2 m                                 | 0,27                             |
|                   | rib configuration | without | 2 m                                 | 0,34                             |
|                   | rib configuration | with    | 2 m                                 | 0,21                             |
| T30               | rib configuration | with    | 2 m                                 | 0,26                             |
| T31               | rib configuration | with    | 2 m                                 | 0,32                             |

TABLE II : TEST RESULTS

| ceiling               | test nr. | $T_1$ hrs | $\alpha$ | $\cotg \beta$ | $\bar{\sigma}/\bar{u}$ [%] | $x/h_o$ | $\Delta h$ in $10^{-3}$ m | $\xi_{\Delta h}$ |
|-----------------------|----------|-----------|----------|---------------|----------------------------|---------|---------------------------|------------------|
| series I<br>without   | T17      | 48        | 1,54     | 4,9           | 8,0                        | 7,5     | 21,4                      | 8,3              |
|                       | T18      | 2,85      | 1,70     | 4,5           | 10,1                       | 6,5     | 52,9                      | 8,8              |
| with                  | T19      | 34        | 1,64     | 4,7           | 8,7                        | 7,1     | 23,6                      | 9,2              |
|                       | T20      | 4,2       | 1,54     | 4,6           | 8,6                        | 7,0     | 58,7                      | 9,3              |
| series II<br>without  | T21      | 40        | 1,55     | 5,0           | 7,7                        | 6,6     | 21,5                      | 7,9              |
|                       | T22      | 1,7       | 1,86     | 3,8           | 13,5                       | 5,5     | 55,7                      | 9,1              |
| with                  | T23      | 40        | 1,60     | 4,6           | 6,8                        | 7,6     | 27,5                      | 10,8             |
|                       | T24      | 3,8       | 1,59     | 4,1           | 10,6                       | 6,4     | 48,5                      | 7,9              |
| series III<br>without | T25      | 9         | 2,57     | 3,3           | 25,2                       | 4,2     | 18,6                      | 11,0             |
|                       | T26      | 15        | 1,94     | 4,2           | 9,8                        | 5,9     | 23,5                      | 9,5              |
|                       | T27      | 4         | 2,04     | 3,8           | 12,7                       | 5,3     | 41,6                      | 11,5             |
|                       | T28      | 0,5       | 2,46     | 3,1           | 17,9                       | 4,0     | 54,4                      | 9,5              |
| with                  | T29      | 4,2       | 2,60     | 3,1           | 22,3                       | 4,0     | 31,0                      | 14,1             |
|                       | T30      | 1,4       | 2,56     | 3,1           | 23,0                       | 3,9     | 53,1                      | 15,2             |
|                       | T31      | 0,48      | 2,58     | 3,0           | 20,7                       | 4,6     | 81,7                      | 15,2             |



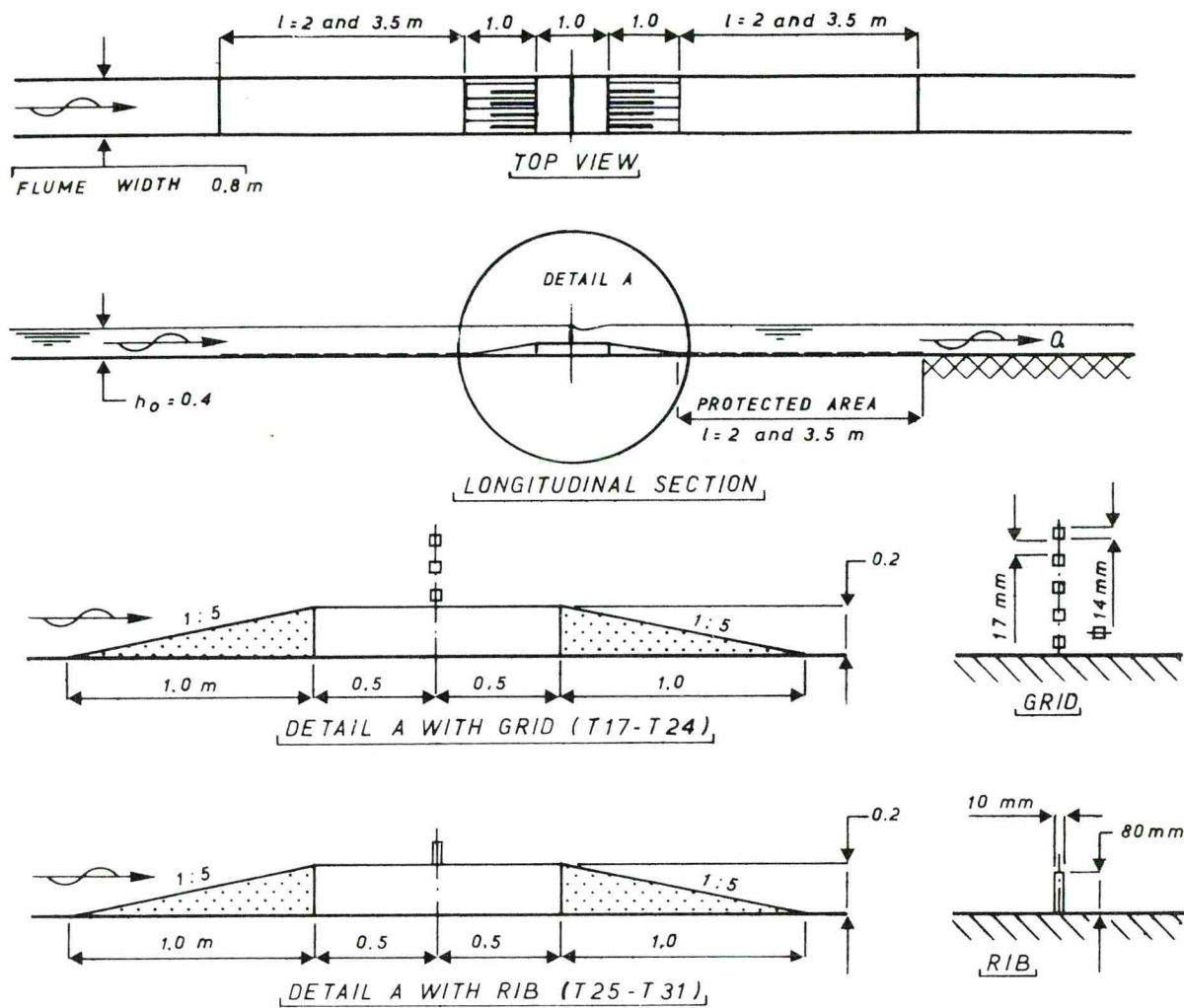


Fig.1 Lay-out and sections with the grid and with the rib configuration.

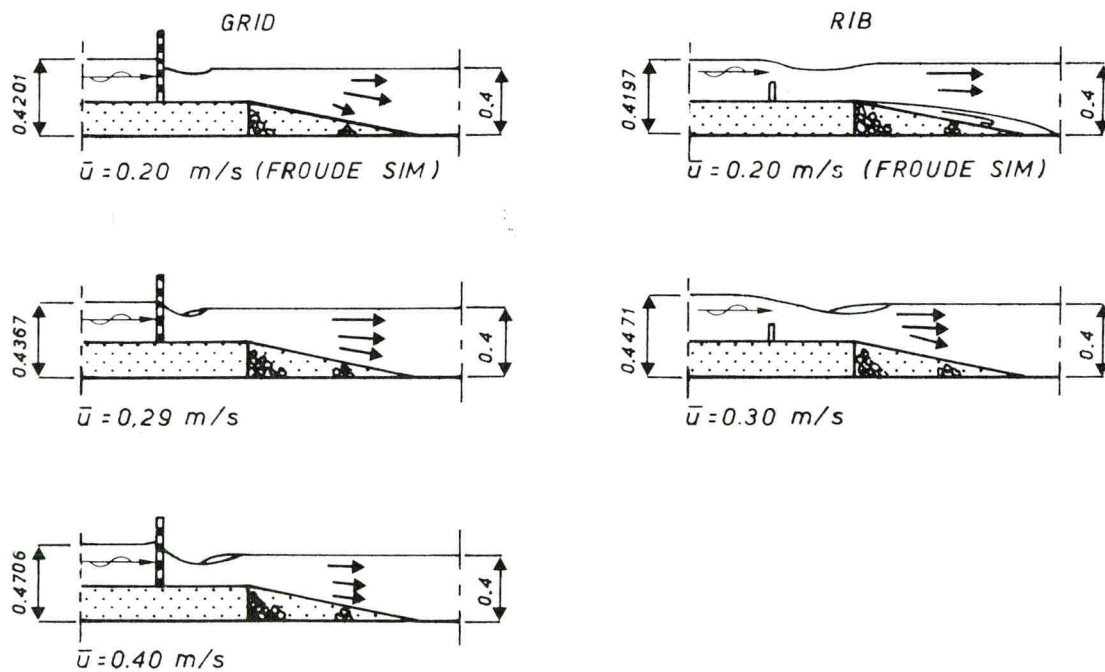


Fig. 2 Water-level variation at Froude similitude and velocity exaggeration condition.

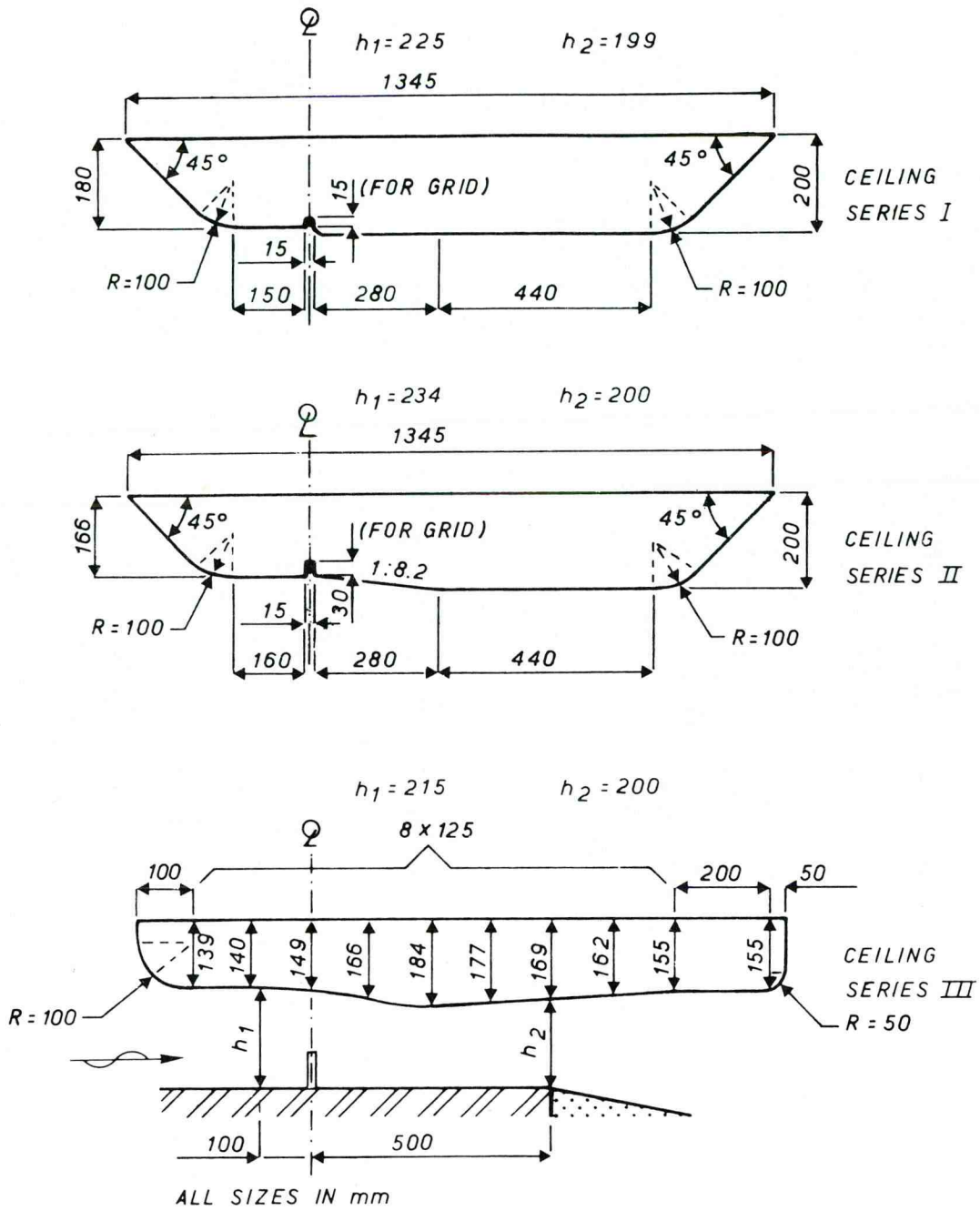


Fig. 3 Ceiling shapes and positions.

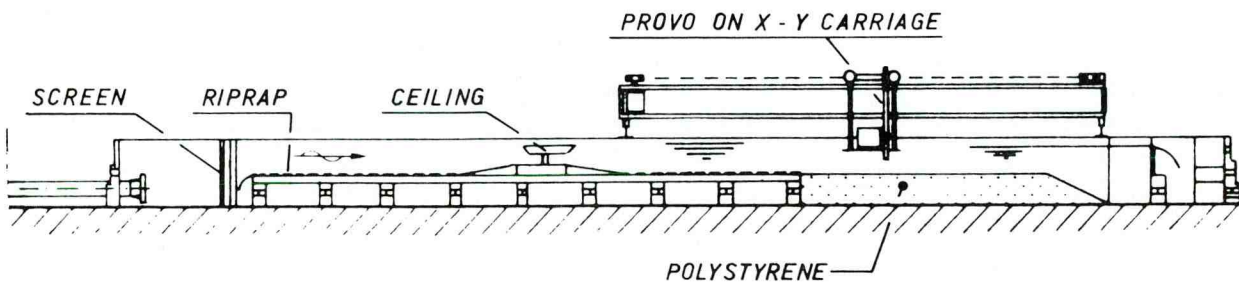


Fig. 4 Longitudinal section of test installation.



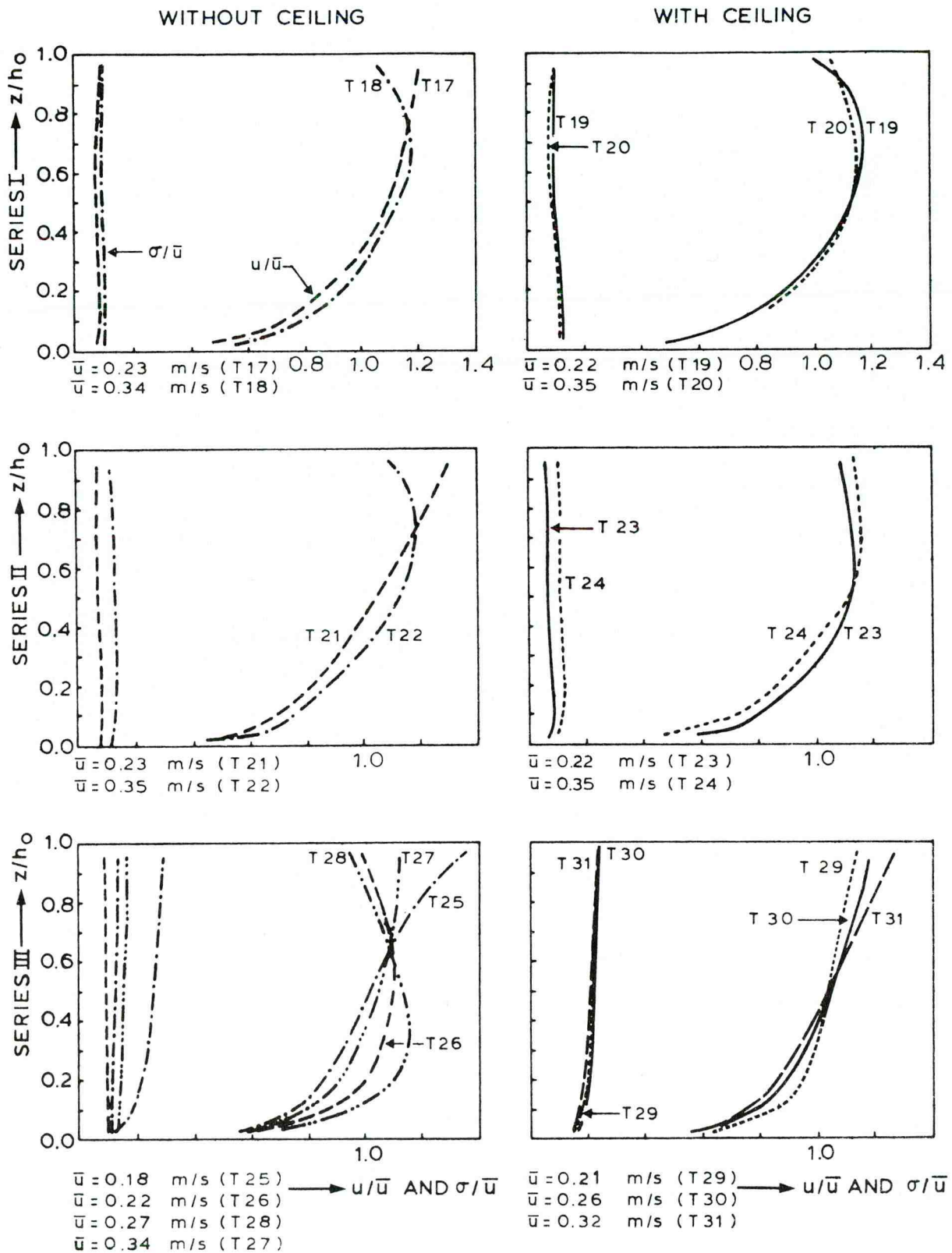


Fig. 5 Velocity and turbulence distributions at the end of the bottom protection.

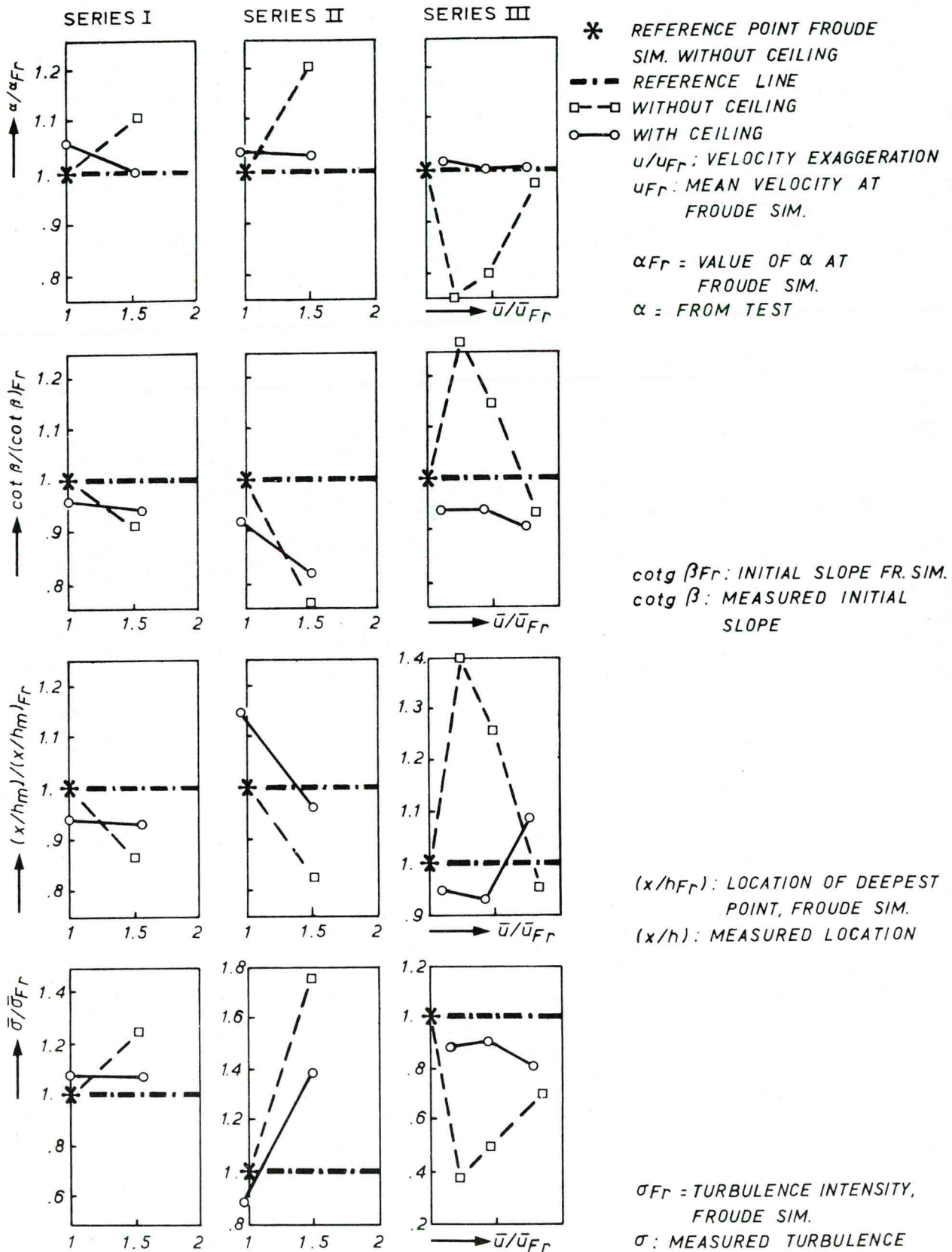
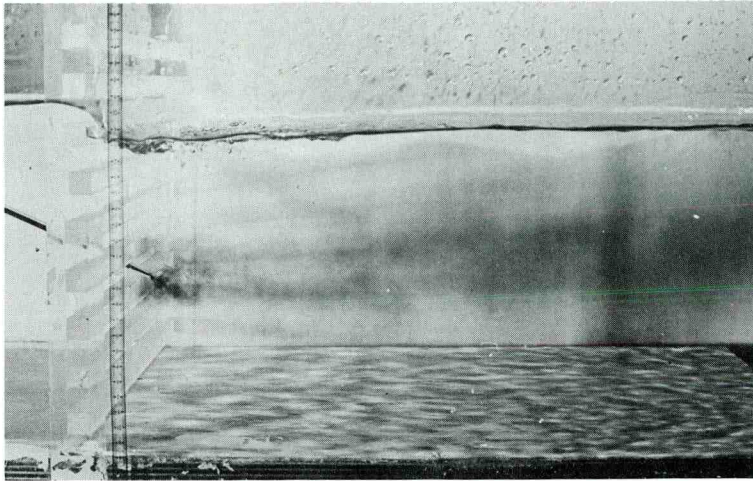


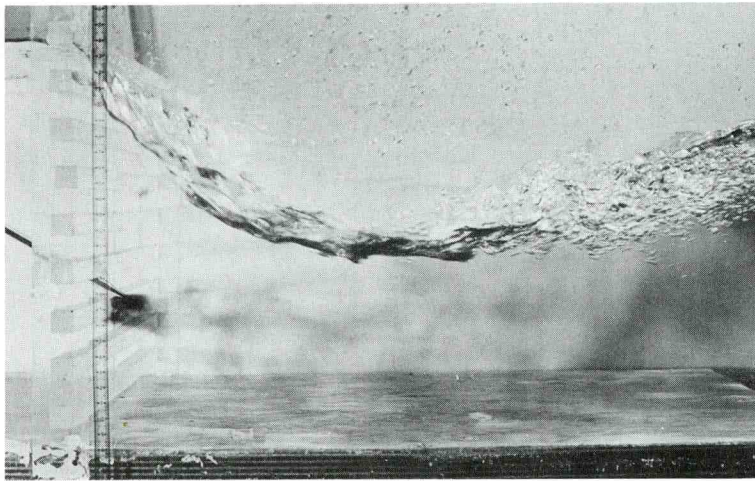
Fig. 6 Test results concerning  $\alpha$ ,  $\beta$ ,  $(x/h_m)$  and  $\sigma$ .



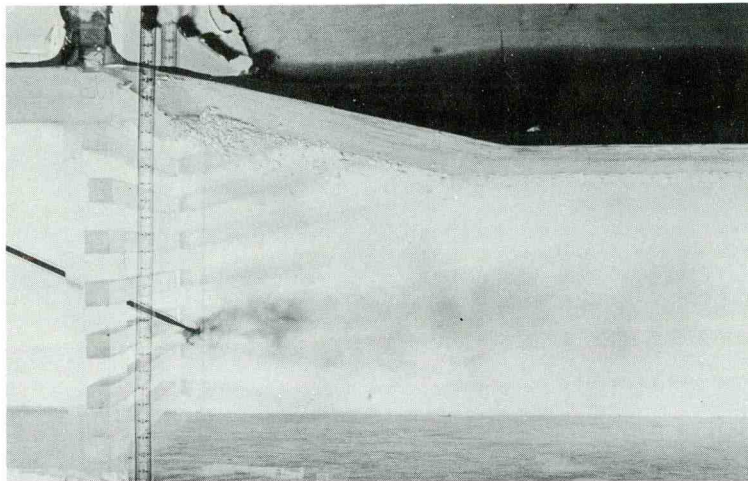
PHOTOGRAPHS



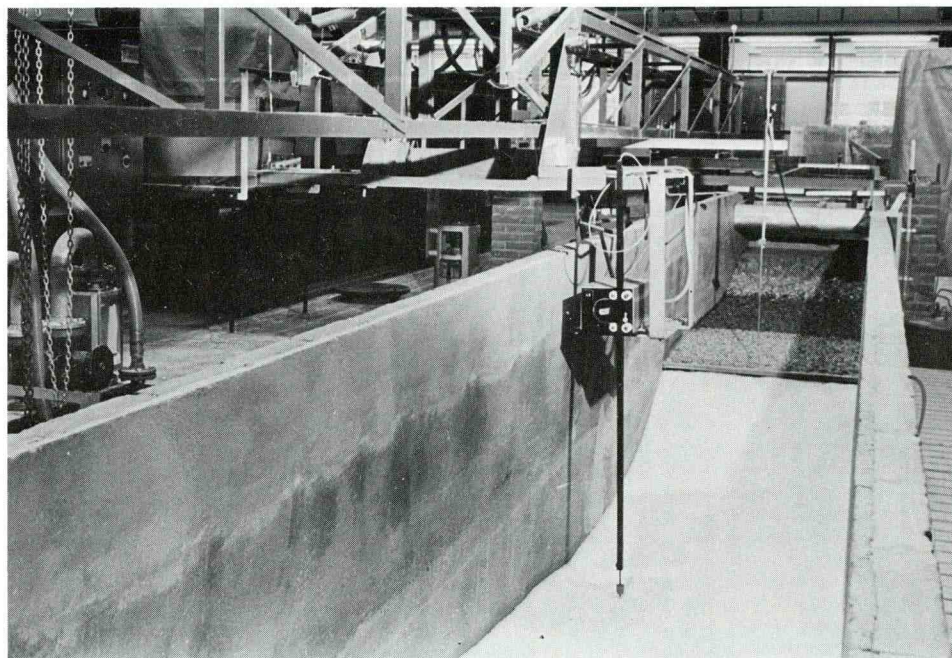
1. Water surface, grid at Froude similarity condition.



2. Water surface, grid with exaggerated velocity.



3. Condition with exaggerated velocity but with ceiling.



4. Overall view of the model and the scoure hole.



p.o. box 177      2600 mh delft      the netherlands